Computers and Mathematics with Applications 62 (2011) 93–108

Contents lists available at ScienceDirect

Computers and Mathematics with Applications

journal homepage: www.elsevier.com/locate/camwa

Diffusion of a chemically reactive species of a power-law fluid past a stretching surface

K. Vajravelu [a,*], K.V. Prasad [b], N.S. Prasanna Rao [c]

[a] Department of Mathematics, University of Central Florida, Orlando, FL 32816, USA

[b] Department of Mathematics, Central College Campus, Bangalore University, Bangalore 560001, India

[c] Department of Mechanical Engineering, RNS Institute of Technology, Channasandra, Bangalore 560061, India

ARTICLE INFO

Article history:
Received 3 June 2010
Received in revised form 20 April 2011
Accepted 20 April 2011

Keywords:
Reactive species
Magnetic field
Power-law fluid
Stretching sheet
Modified Schmidt number
Sherwood number

ABSTRACT

A numerical solution for the steady magnetohydrodynamic (MHD) non-Newtonian power-law fluid flow over a continuously moving surface with species concentration and chemical reaction has been obtained. The viscous flow is driven solely by the linearly stretching sheet, and the reactive species emitted from this sheet undergoes an isothermal and homogeneous one-stage reaction as it diffuses into the surrounding fluid. Using a similarity transformation, the governing non-linear partial differential equations are transformed into coupled nonlinear ordinary differential equations. The governing equations of the mathematical model show that the flow and mass transfer characteristics depend on six parameters, namely, the power-law index, the magnetic parameter, the local Grashof number with respect to species diffusion, the modified Schmidt number, the reaction rate parameter, and the wall concentration parameter. Numerical solutions for these coupled equations are obtained by the Keller–Box method, and the solutions obtained are presented through graphs and tables. The numerical results obtained reveal that the magnetic field significantly increases the magnitude of the skin friction, but slightly reduces the mass transfer rate. However, the surface mass transfer strongly depends on the modified Schmidt number and the reaction rate parameter; it increases with increasing values of these parameters. The results obtained reveal many interesting behaviors that warrant further study of the equations related to non-Newtonian fluid phenomena, especially shear-thinning phenomena. Shear thinning reduces the wall shear stress.

1. Introduction

During the past three decades, the study of heat, mass, and momentum transfer in boundary layer flow over a continuously moving surface through a quiescent liquid has attracted considerable attention. This interest is due to several important applications in electrochemistry and polymer processing (see [1,2]) industries. Flows due to a continuously moving surface are often encountered in the aerodynamic extrusion of plastic sheets, the boundary layer along liquid film in condensation processes, the cooling and drying of papers and textiles, and glass fiber production. In view of these applications, Sakiadis [3] initiated a theoretical study for the momentum transfer occurring in the boundary layer adjacent to a continuous surface moving steadily through an otherwise quiescent fluid environment, and this was experimentally verified by Tsou et al. [4]. Crane [5] extended the work of Sakiadis by assuming that the velocity of the sheet varies linearly with the distance from the slit. Thereafter, numerous investigations were made on the stretching sheet problem with linear

* Corresponding author.
E-mail address: vajravel@mail.ucf.edu (K. Vajravelu).

0898-1221/$ – see front matter © 2011 Elsevier Ltd. All rights reserved.
doi:10.1016/j.camwa.2011.04.055

Nomenclature

b	Stretching rate, a positive constant
B_0	Magnetic field
C	Species concentration in the fluid
C_w	Species concentration near the plate
C_f	Skin friction
C_∞	Species concentration with fluid far away form the plate
D	Chemical molecular diffusivity
E	Constant
f	Dimensionless velocity variable
g	Acceleration due to gravity
Gc_x	Modified Grashof number
$h(x)$	Heat transfer coefficient
H_0	Applied transverse magnetic field
k_1	Chemical reaction parameter
l	Characteristic length
Mn	Magnetic parameter
n	Power-law index
Nsc	Generalized modified Schmidt number for power-law fluids
Re_x	Local Reynolds number
r	Species concentration parameter
$\mathrm{Sh}_w(x)$	Sherwood number
x	Horizontal distance
y	Vertical distance
u	Velocity in the x-direction
U	Velocity of the sheet
v	Velocity in the y-direction

Greek symbols

β^*	Coefficient of expansion with concentration
β	Chemical reaction rate parameter
η	Similarity variable
γ	Kinematic viscosity
ψ	Stream function
ρ	Density
σ	Electrical conductivity
τ_{xy}, τ_{ij}	Shear stress
ϕ	Dimensionless concentration variable
δ_{ij}	Kronecker delta
μ^*	Consistency index of the power-law fluid

Subscripts

w, ∞	Conditions at the surface and in the free stream
η	Differentiation with respect to η

stretching under different physical situations [6–9]. It is well known that a number of industrial fluids such as molten plastics, polymeric liquids, and foodstuffs (or slurries) exhibit non-Newtonian fluid behavior. Therefore, heat and mass transfer in non-Newtonian fluids is of practical importance. Many different types of non-Newtonian fluid exist, but the simplest and most common type is the power-law fluid for which the rheological equation of state between the stress components τ and strain components e is defined by (see [10])

$$\tau_{ij} = -P\delta_{ij} + K\left|\sum\sum e_{lm}e_{lm}\right|^{\frac{n-1}{2}} e_{ij},$$

where P is the pressure, δ_{ij} is the Kronecker delta, and K and n are respectively the consistency and the flow behavior indices of the fluid. Such fluids are known as power-law fluids. For $n > 1$, the fluid is said to be a dilatant or shear-thickening fluid; for $n < 1$, the fluid is called a shear-thinning or pseudo-plastic fluid, and for $n = 1$, the fluid is simply a Newtonian fluid. Several studies in the literature suggest the range $0 < n < 2$ for the value of power-law index n. Schowalter [11]

studied the application of boundary layer theory to pseudo-plastic fluids. Acrivos et al. [12] investigated the momentum and heat transfer in the laminar boundary layer flow of non-Newtonian fluids past external surfaces. Similarity solutions for non-Newtonian power-law fluids were obtained by Lee and Ames [13]. Andersson and Dandapat [14] studied the flow of a power-law fluid over a stretching sheet. Sahoo et al. [15] considered the momentum and heat transfer in a power-law fluid from a continuous moving plate with non-uniform surface velocity distributions.

Even though the above-mentioned papers do not consider the situations where hydromagnetic effects arise, in recent years, we find several applications in the polymer industry (where one deals with stretching of plastic sheets) and metallurgy where hydromagnetic techniques are being used. To be more specific, it may be pointed out that many metallurgical processes involve the cooling of continuous strips or filaments by drawing them through a quiescent fluid, and that, in the process of drawing, these strips are sometimes stretched. Mention may be made of drawing, annealing, and thinning of copper wires. In all these cases, the properties of the final product depend to a great extent on the rate of cooling by drawing such strips in an electrically conducting fluid subject to a uniform magnetic field. Another important application of hydromagnetic flows to metallurgy lies in the purification of molten metals from non-metallic inclusions by the application of a magnetic field. In view of this, the study of the magnetohydrodynamic (MHD) flow of a non-Newtonian fluid over a stretching sheet has been carried out by many researchers [16–21]. By taking the advantage of the mathematical equivalence of the thermal boundary layer problem with the concentration analog, results obtained for the heat transfer characteristics can be carried directly over to the case of mass transfer by replacing the Prandtl number with the Schmidt number. However, the presence of a chemical reaction term in the mass diffusion equation generally destroys the formal equivalence with the thermal energy problem, and, moreover, generally prohibits the construction of similarity solutions. Therefore, the study of heat and mass transfer with a chemical reaction is of great practical importance to engineers and scientists because of its almost universal occurrence in many branches of science and engineering. The effects of a chemical reaction depend on whether the reaction is heterogeneous or homogeneous. This depends on whether the reactions occur at an interface or as a single-phase volume reaction. A reaction is said to be of first order if the rate of reaction is directly proportional to the concentration. All industrial chemical processes are designed to transform cheaper raw materials to high-value products, usually via a chemical reaction.

The first step in any reaction engineering analysis is formulating a mathematical framework to describe the rate and mechanisms by which one chemical species is converted into another in the absence of any transport limitations (chemical kinetics). Analysis of the transport processes and their interaction with chemical reactions can be quite difficult, and is intimately connected to the underlying fluid dynamics. Such a combined analysis of chemical and physical processes constitutes the core of chemical reaction engineering. In many industrial processes involving flow and mass transfer over a moving surface, the diffusing species can be generated or absorbed due to some kind of chemical reaction with the ambient fluid [22]. This generation or absorption of species can affect the flow and accordingly the properties and quality of the final product. Hence, it is important to take into account the effect of the chemical reaction in addition to the effect of diffusion of the species in analyzing the mass transfer phenomenon. The available literature [23–29] on flow and mass transfer reveals that not much work has been carried out for power-law fluids. Recently, Cortell [29] investigated the MHD flow and mass diffusion of chemical species with first-order and higher-order reactions of an electrically conducting fluid of second grade in a porous medium over a stretching surface.

The physical situation described in all the above studies is related to the flow and mass transfer characteristics over a stretching sheet. In the present investigation, we are interested in modeling the steady two-dimensional boundary layer flow and mass transfer of a non-Newtonian power-law fluid induced by a flat surface. This is a generalization of the work of Andersson et al. [16] to the case of MHD flow over a stretching sheet in the presence of species concentration and a chemical reaction. The presence of the power-law index and the chemical reaction term in the momentum and the mass diffusion equations leads to coupled, non-linear partial differential equations (PDEs). These PDEs are converted to coupled non-linear ordinary differential equations (ODEs). To deal with the coupling and the non-linearity in the boundary value problem, a numerical finite difference scheme called the Keller–Box method is adopted. The results are analyzed for several sets of values of the governing parameters on the flow and mass transfer characteristics.

2. Mathematical analysis

Let us consider the steady incompressible flow of a viscous electrically conducting power-law fluid over a stretching sheet with a magnetic field of strength B_0 (applied normal to the surface), as shown in Fig. 1. The flow is generated due to the stretching of the sheet (caused by the simultaneous application of two equal and opposite forces along the x-axis, keeping the origin fixed). The continuous stretching sheet is assumed to have a linear velocity $U(x) = bx$ and species diffusion $C_w(x) = C_\infty + E\left(\frac{x}{l}\right)^r$, where b is the linear stretching rate, x is the distance from the slit, E is a constant whose value depends upon the properties of the fluid, r is the species concentration parameter, and l is the characteristic length. An appropriate mass transfer analog to the problem would be the flow along a flat plate that contains a species A that is slightly soluble in fluid B. The concentration at the plate surface would be C_w, and the solubility of A in B and the concentration of species A far away from the plate would be C_∞. Let the reaction of species A with B be a first-order homogeneous chemical reaction with rate constant k_1. It is desired to analyze the system by the boundary layer method. It is assumed that the concentration of the dissolved A is small enough and the physical properties ρ, γ, and D are virtually constant throughout the fluid. It is also assumed that the magnetic Reynolds number Re_m is very small, i.e., $\mathrm{Re}_m = \mu_0\sigma bl \ll 1$, where μ_0 is

the magnetic permeability and σ is the electric conductivity. Further, since there is no electric field, the electric field due to polarization of charges is negligible. Under these assumptions, and invoking the usual boundary layer approximations, the flow can be shown to be governed by the following system of coupled partial differential equations along with the necessary conditions:

$$\frac{\partial u}{\partial x}+\frac{\partial v}{\partial y}=0, \tag{2.1}$$

$$u\frac{\partial u}{\partial x}+v\frac{\partial u}{\partial y}=-\gamma\frac{\partial}{\partial y}\left(-\frac{\partial u}{\partial y}\right)^{n}-\frac{\sigma B_0^2}{\rho}u+g\beta^{*}\left(C-C_{\infty}\right), \tag{2.2}$$

$$u\frac{\partial C}{\partial x}+v\frac{\partial C}{\partial y}=D\frac{\partial^2 C}{\partial y^2}-k_1C, \tag{2.3}$$

$$u(x,0)=U(x)=bx, \tag{2.4a}$$

$$v(x,0)=0, \tag{2.4b}$$

$$C(x,0)=C_w(x)\left[=C_{\infty}+E\left(\frac{x}{l}\right)^{r}\right], \tag{2.4c}$$

$$u(x,y)\to 0,\qquad C(x,y)\to C_{\infty}\quad \text{as } y\to\infty. \tag{2.4d}$$

In the above equations, u and v are the velocity components along the x-axis and the y-axis, respectively. γ is the kinematic viscosity of the fluid, n is the power-law index, ρ is the fluid density, g is the acceleration due to gravity, β^* is the volumetric concentration coefficient, D is the chemical molecular diffusion coefficient of the diffusing species in the fluid, and k_1 denotes the reaction rate constant of a first-order homogeneous and irreversible reaction. A rigorous derivation together with the subsequent analysis of the boundary layer equations for power-law fluids was recently provided by Denier and Dabrowski [30]. They focused on boundary layer flow driven by a free stream, $U(x)\approx x^m$, i.e., Falkner–Skan type. Such boundary layer flows are driven by a stream-wise pressure gradient $-\frac{dp}{dx}=\rho\frac{du}{dx}$ set up by the external free stream, outside the viscous boundary layer. In the present context, no driving pressure gradient is present. Instead, the flow is driven solely by a flat surface, which moves with a prescribed velocity $U(x)=bx$. The first term in the right-hand side of Eq. (2.2), the shear rate, is assumed to be negative throughout the boundary layer since the stream-wise velocity component u decreases monotonically with the distance y from the moving surface (for a continuous stretching surface). Here, Eq. (2.4d) claims that the stream-wise velocity and the species diffusion vanish outside the boundary layer, Eq. (2.4c) is the species concentration of the reactant which is maintained at a prescribed surface value C_w and is assumed to vary as a function of x, and the requirement Eq. (2.4b) signifies the importance of the impermeability of the stretching surface, whereas Eq. (2.4a) ensures no slip at the surface. As in [13], the following transformation is introduced:

$$\eta=\frac{y}{x}(\mathrm{Re}_x)^{\frac{1}{n+1}},\qquad \psi(x,y)=Ux(\mathrm{Re}_x)^{\frac{-1}{n+1}}f(\eta),\qquad \phi(\eta)=\frac{C-C_{\infty}}{C_w-C_{\infty}}, \tag{2.5}$$

where η is the similarity variable, $\psi(x,y)$ is the stream function, and f and ϕ are the dimensionless similarity function and mass concentration, respectively. The velocity components u and v are given by

$$u=\frac{\partial\psi}{\partial y}\qquad v=-\frac{\partial\psi}{\partial x}. \tag{2.6}$$

The local Reynolds number is defined by

$$\mathrm{Re}_x=\frac{U^{2-n}x^n}{\gamma}. \tag{2.7}$$

The mass conservation equation (2.1) is automatically satisfied by Eq. (2.6). By assuming the similarity function f to depend on the similarity variable η, the momentum equation (2.2) and the mass transfer equation (2.3) transform into a coupled non-linear ordinary differential equation:

$$n(-f'')^{n-1}f'''-f'^2+\left(\frac{2n}{n+1}\right)ff''-\mathrm{Mn}f'+Gc_x\phi=0 \tag{2.8}$$

$$\phi''+NSc\left(\frac{2n}{n+1}f\phi'-rf'\phi\right)=\beta Nsc\phi, \tag{2.9}$$

where $\mathrm{Mn}=\frac{\sigma B_0^2}{\rho b}$ is the magnetic parameter, $Gc_x=\frac{g\beta^*(C_w-C_{\infty})xb^{-n}}{\gamma\mathrm{Re}_x}$ is the local modified Grashof number with respect to species diffusion, $NSc=\frac{bx^2}{D}(\mathrm{Re}_x)^{\frac{2}{n+1}}$ is the modified Schmidt number for power-law fluids, and $\beta=\frac{k_1}{b}$ is the reaction rate

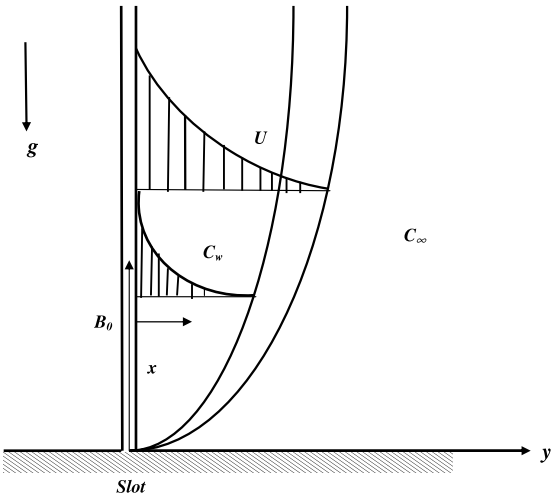

Fig. 1. Physical model and coordinate system.

parameter. Eqs. (2.8) and (2.9) are solved numerically subject to the following transformed boundary conditions obtained from Eq. (2.4) using (2.5). The conditions are

$$f = 0 \quad \text{at } \eta = 0 \tag{2.10a}$$

$$f' = 1 \quad \text{at } \eta = 0, \tag{2.10b}$$

$$\phi = 1 \quad \text{at } \eta = 0, \tag{2.10c}$$

$$f' \to 0, \qquad \phi \to 0 \quad \text{as } \eta \to \infty. \tag{2.10d}$$

It should be noted that the velocity $U = U(x)$ is used to define the dimensionless stream function f in Eq. (2.5) and the local Reynolds number in Eq. (2.7) describes the velocity of the moving surface that drives the flow. This choice is in contrast to conventional boundary layer analysis, in which the free stream velocity is taken as the velocity scale. Although the transformation defined in Eqs. (2.5) and (2.7) can be used for any arbitrary variation of $U(x)$, the transformation results in a true similarity problem only if U varies as bx. Such surface velocity variations are therefore required for the ordinary differential equation (2.8) to be valid. Non-similar stretching sheet problems which require the solution of partial differential equations rather than ordinary differential equations were considered by several researchers for Newtonian fluids. We noticed that in the absence of mass transfer and a magnetic parameter, Eqs. (2.8) and (2.9) reduce to those of Andersson and Dandapat [14], while for a Newtonian fluid ($n = 1$) in the presence of mass transfer, the equations reduce to those of Andersson et al. [26]. Also, in the presence of a magnetic parameter for the power-law fluid flow, without mass transfer, the Eq. (2.8) reduces to those of Cortell [18] and Andersson et al. [31].

The physical quantities of interest include the velocity components u and v, the skin friction coefficient C_{f_x} and the mass transfer rate $\mathrm{Sh}_w(x)$ at the wall. In terms of the transformation variables, these quantities can be written as

$$u = Uf', \tag{2.11}$$

$$v = -U(\mathrm{Re}_x)^{\frac{-1}{n+1}}\left[\frac{2n}{n+1}f + \eta\left(\frac{1-n}{1+n}\right)f'\right] \tag{2.12}$$

$$\frac{1}{2}C_f[\mathrm{Re}_x]\frac{1}{n+1} = [-f''(0)]^n \tag{2.13}$$

$$\mathrm{Sh}_x\mathrm{Re}_x^{\frac{-1}{n+1}} = -\phi'(0). \tag{2.14}$$

3. Numerical procedure

The system of transformed coupled non-linear ordinary differential equations (2.8) and (2.9) together with the boundary conditions (2.10) is solved numerically by an efficient finite difference scheme known as the Keller–Box method [31–33] for different values of the physical parameters. The numerical solutions are obtained in four steps, as follows.

- Reduce Eqs. (2.8) and (2.9) to a system of first-order equations;
- write the difference equations using central differences;

Table 1
Comparison of skin friction $f''(0)$ values with those of Andersson et al. [31] and Cortell [18] for $Gc_x = 0.0$.

	Mn	$n = 0.4$	$n = 0.6$	$n = 0.8$	$n = 1.0$	$n = 1.2$	$n = 2.0$
Andersson et al. [31]		−1.273	−1.096	−1.029	−1.000	−0.987	−0.980
Cortell [18]	0.0	−1.2730	–	–	−1.000	–	−0.9797
Present results		−1.27345	−1.09838	−1.02897	−1.000	−0.98738	−0.98035
Andersson et al. [31]		−1.851	−1.4649	−1.3086	−1.2247	−1.1752	−1.0926
Cortell [18]	0.5	−1.8111	–	–	−1.2247	–	−1.0296
Present results		−1.8154	−1.4649	−1.3086	−1.2247	−1.1754	−1.0926

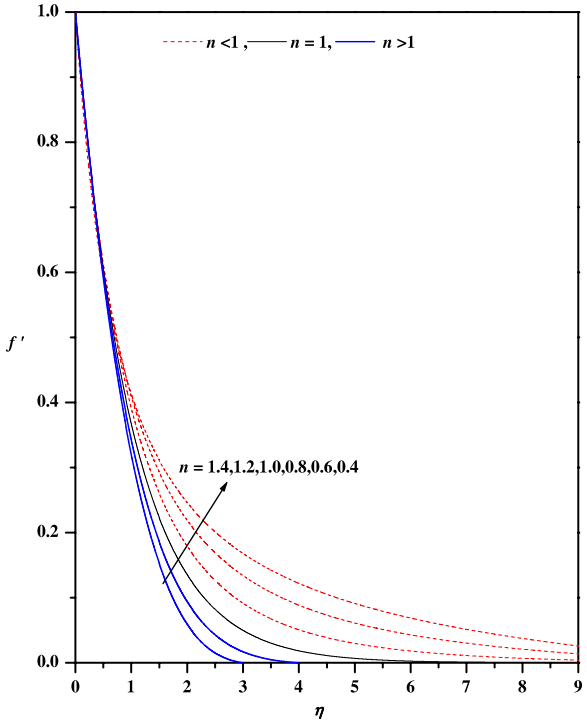

Fig. 2a. Velcoity profiles for different values of n with Mn $= 0.0$ and $Gc_x = 0.0$.

- linearize the algebraic equations by Newton's method, and write them in matrix-vector form; and
- solve the linear system by the block tridiagonal elimination technique.

For the sake of brevity, further details on the solution process are not presented here. It is also important to note that the computational time for each set of input parameter values should be short. Because the physical domain in this problem is unbounded, whereas the computational domain has to be finite, we apply the far-field boundary conditions for the similarity variable η at a finite value denoted by $\eta_{\max}$. We ran our bulk computations with the value $\eta_{\max} = 10$, which is sufficient to achieve the far-field boundary conditions asymptotically for all values of the parameters considered. For the numerical calculations, a uniform step size of $\Delta\eta = 0.01$ is found to be satisfactory, and the solutions are obtained with an error tolerance of 10^{-6} in all cases. To assess the accuracy of the present method, a comparison of the skin friction between the present results and previously published results is made, for a special case (no mass transfer), and is shown in Table 1.

4. Results and discussion

In order to have an insight into the effects of the parameters on the MHD flow and mass transfer characteristics, we present the numerical results graphically in Figs. 2–5 and in Tables 2 and 3 for several sets of values of the parameters. Velocity profiles are presented in Figs. 2a–2d and concentration species distribution profiles are depicted in Figs. 3–5.

We can have a glimpse of the physical layout of the boundary layer structure which develops near the slit by observing the horizontal velocity profiles in Figs. 2a–2d. Figs. 2a–2d illustrate the effects of the power-law index n, magnetic parameter Mn, and modified Grashof number Gc_x on the horizontal velocity f'. It is noticed from the Fig. 2a that the velocity profile f' decreases with increasing values of n in the boundary layer, but this effect is not very prominent near the wall. The effect of increasing values of n is to reduce the velocity, thereby reducing the boundary layer thickness, i.e., the thickness is much larger for shear-thinning (pseudo-plastic) fluids ($0 < n < 1$) than for Newtonian ($n = 1$) and shear-thickening

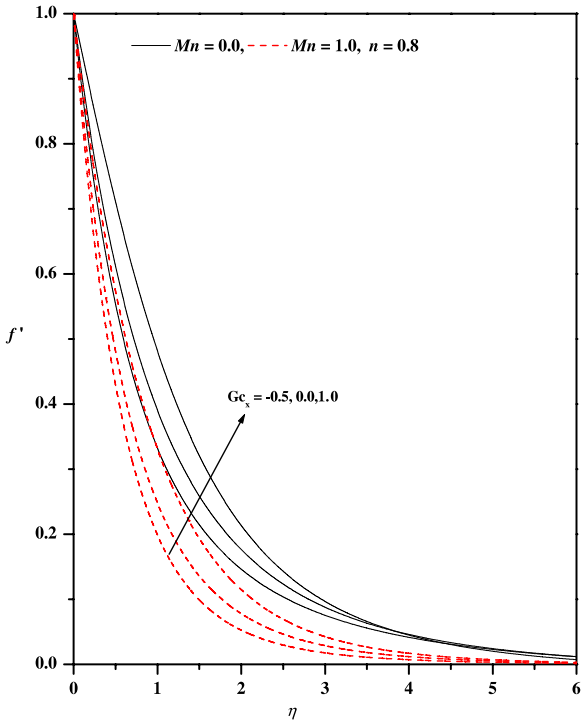

Fig. 2b. Velocity profiles for different values of Gc_x and Mn with $NSc = 1.0$, $r = 1.0$, and $\beta = 1.0$.

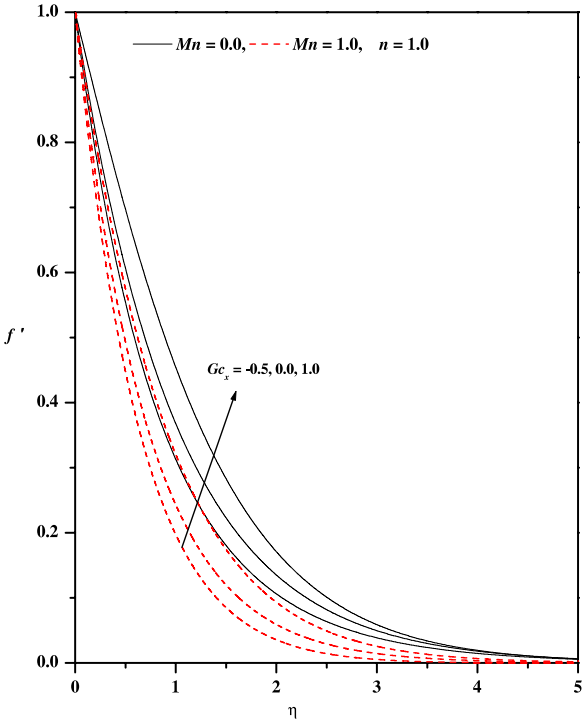

Fig. 2c. Velocity profiles for different values of Gc_x and Mn with $NSc = 1.0$, $r = 1.0$, and $\beta = 1.0$.

(dilatant) fluids ($1 < n < 2$), as clearly seen in Fig. 2a. The effect of the magnetic parameter Mn and modified Grashof number Gc_x on the velocity f' is depicted in Figs. 2b–2d. It is observed that the f' decreases with an increase in Mn due to the fact that the introduction of a transverse magnetic field, normal to the flow direction, has a tendency to create a drag, known as the Lorentz force, which tends to resist the flow. This behavior occurs in all three cases, namely, shear-thickening,

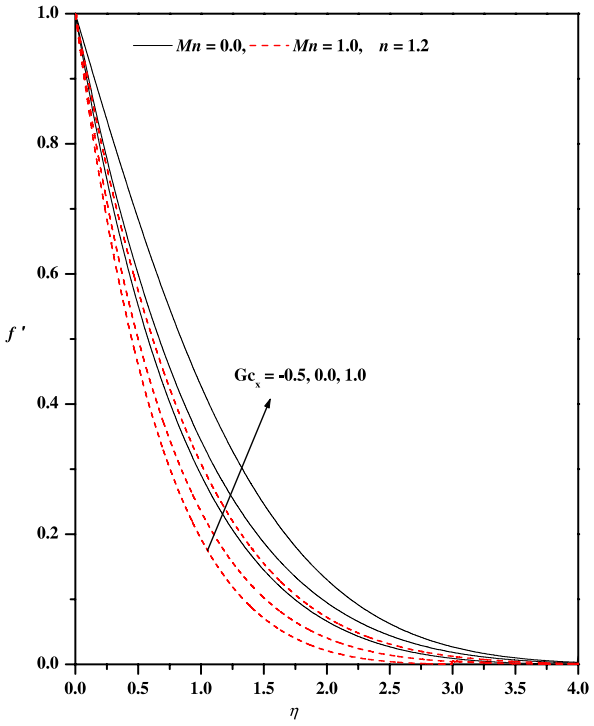

Fig. 2d. Velocity profiles for different values of Gc_x and Mn with $NSc = 1.0$, $r = 1.0$, and $\beta = 1.0$.

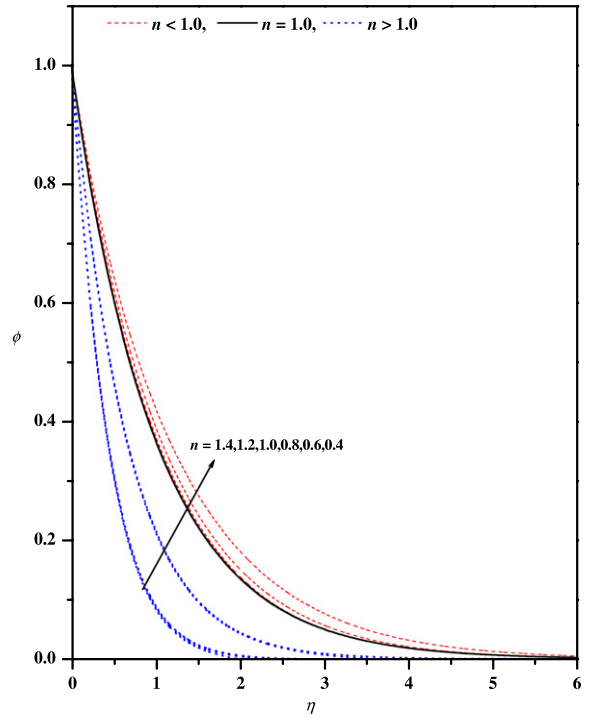

Fig. 3a. Concentration profiles ϕ versus η for different values of n with $Gc_x = 0.0$ and Mn $= 0.0$.

Newtonian and shear-thinning fluids. These results are consistent with the results of Anderson et al. [31]. An increase in the value of Gc_x leads to an increase in the mass transfer gradient. This leads to the enhancement of the velocity profile f' due to the enhanced species diffusion, and thus increases the boundary layer thickness. This behavior can also be seen in Newtonian fluids for $n = 1$, shear-thinning (pseudo-plastic) fluids for $n < 1$, and shear-thickening (dilatant) fluids for

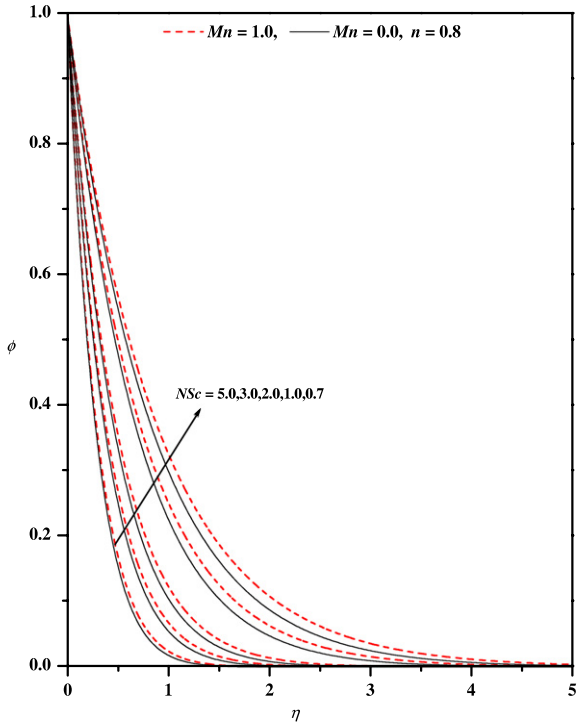

Fig. 3b. Concentration profiles ϕ versus η for different values of NSc and Mn with $Gc_x = 0.0$, $r = 1.0$, and $\beta = 1.0$.

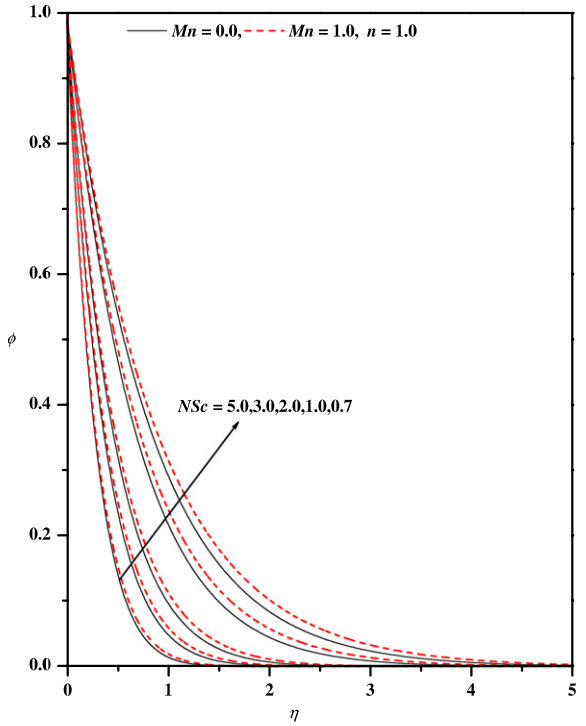

Fig. 3c. Concentration profiles ϕ versus η for different values of NSc and Mn with $Gc_x = 0.0$, $\beta = 1.0$, and $r = 1.0$.

$n > 1$ (see Figs. 2b–2d, respectively). Figs. 2b–2d reveal that the boundary layer thickness is larger for shear-thinning fluids as compared to Newtonian and shear-thickening fluids.

The graphs for the species concentration distribution ϕ for several sets of values of the non-dimensional parameters are presented in Figs. 3–5. The general trend from the concentration profiles ϕ shows that the species distribution is unity

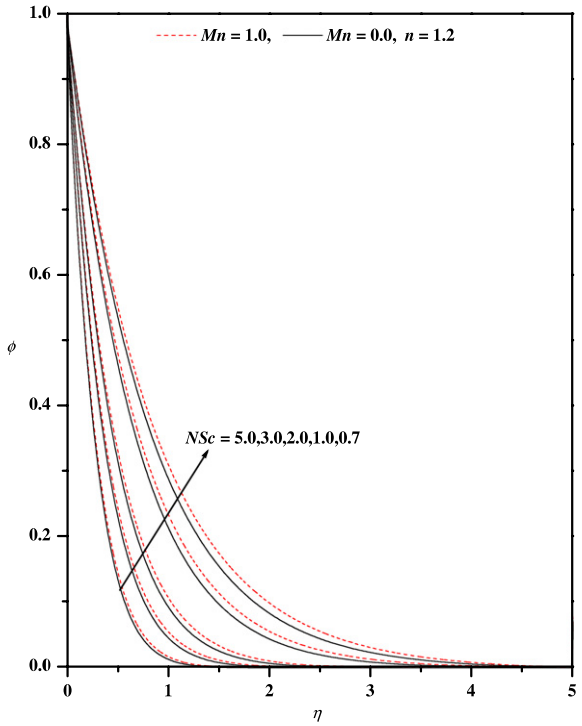

Fig. 3d. Concentration profiles ϕ versus η for different values of NSc and Mn with $Gc_x = 0.0$, $\beta = 1.0$, and $r = 1.0$.

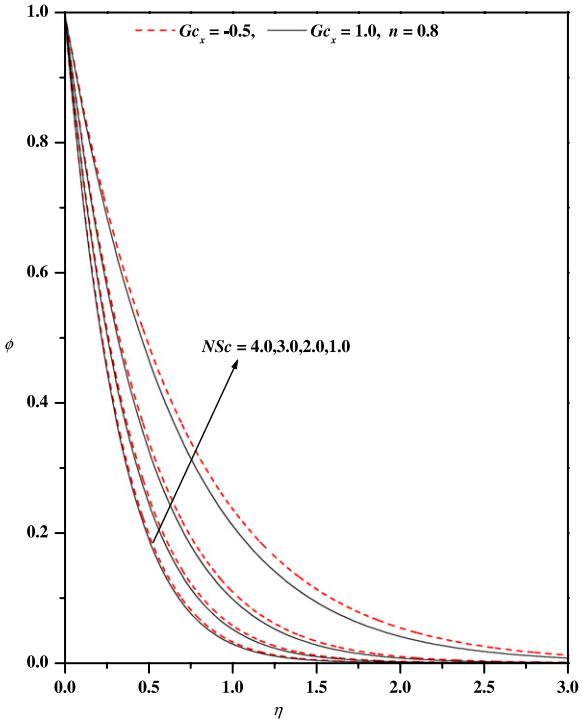

Fig. 4a. Concentration profiles ϕ versus η for different values of NSc and Gc_x with Mn $= 0.0$, $\beta = 1.0$, and $r = 1.0$.

at the wall with the change of physical parameters and tends asymptotically to zero as the distance increases from the boundary. The effect of the power-law index, n, on the concentration species distribution ϕ in the boundary layer is shown in Fig. 3a. The effect of an increase in the values of n leads to thinning of the species distribution boundary layer. This behavior is very noticeable in shear-thinning and shear-thickening fluids. In Figs. 3b–3d, the profiles for the concentration

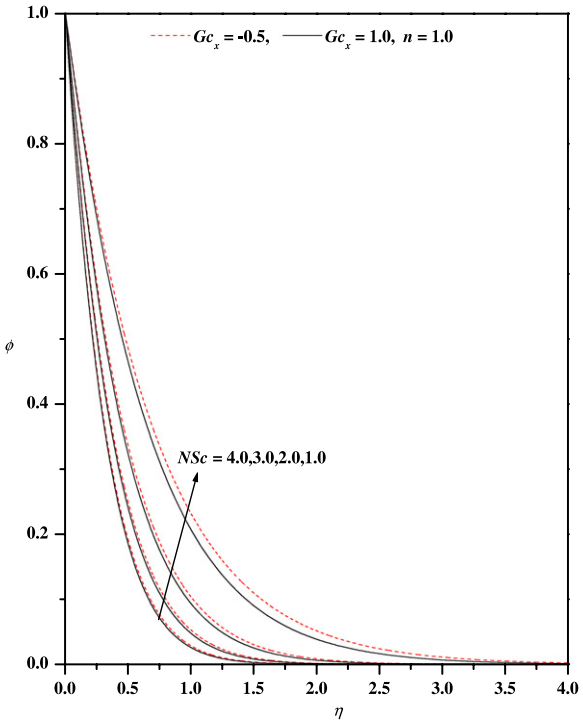

Fig. 4b. Concentration profiles ϕ versus η for different values of NSc and Gc_x with Mn $= 0.0$, $\beta = 1.0$, and $r = 1.0$.

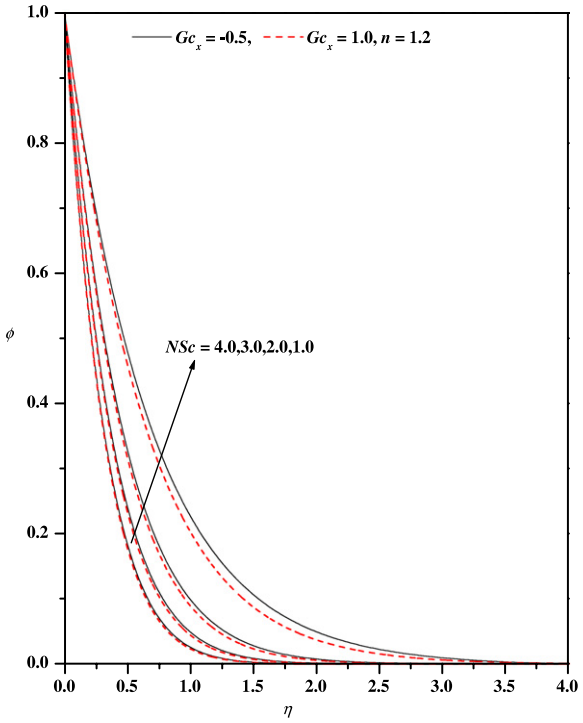

Fig. 4c. Concentration profiles ϕ versus η for different values of NSc and Gc_x with Mn $= 0.0$, $\beta = 1.0$, and $r = 1.0$.

species distribution ϕ are plotted for different values of modified Schmidt number NSc in the presence/absence of Mn for shear-thinning (Fig. 3b), Newtonian (Fig. 3c), and shear-thickening (Fig. 3d) fluids. It is observed that an increase in Mn leads to an increase in the concentration. This is because the Lorentz force increases the friction between the layers, and this is responsible for an increase in concentration ϕ. However, an increase of the value of the modified Schmidt number Nsc leads

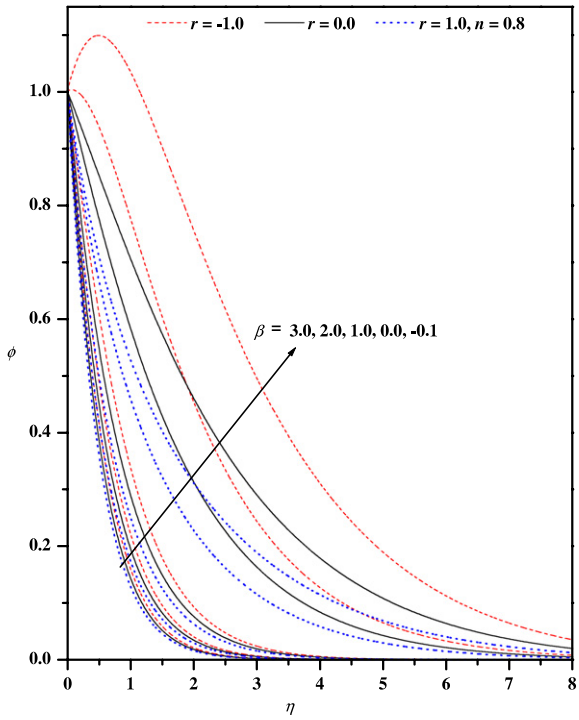

Fig. 5a. Concentration profiles ϕ versus η for different values of r and β with $Gc_x = 0.0$, Mn $= 1.0$, and $NSc = 1.0$.

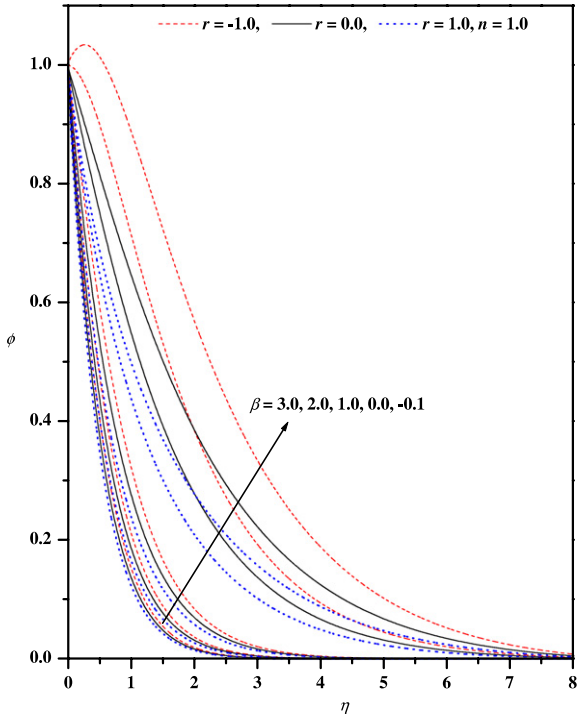

Fig. 5b. Concentration profiles ϕ versus η for different values of β and r with $Gc_x = 0.0$, $NSc = 1.0$, and Mn $= 1.0$.

to a decrease of the thickness of the concentration boundary layer. This is due to the thinning of the concentration boundary layer with the introduction of species diffusion. This phenomenon occurs for shear-thickening (see Fig. 3b), Newtonian (see Fig. 3c), and shear-thinning (see Fig. 3d) fluids. By comparing these figures, we see that the concentration boundary layer thickness is larger for shear-thinning fluids than for the Newtonian and shear-thickening fluids.

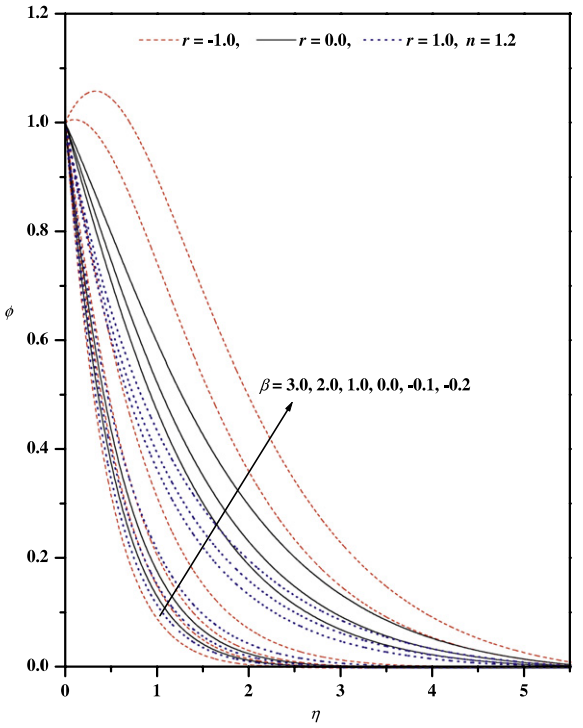

Fig. 5c. Concentration profiles ϕ versus η for different values of β and r with $Gc_x = 1.0$, Mn $= 1.0$, and $NSc = 1.0$.

Table 2
Skin friction and mass transfer gradient for several sets of values of the physical parameters.

Nsc	β	r	Mn	Gc_x	$n = 0.8$		$n = 1.0$		$n = 1.2$	
					$f''(0)$	$\varphi'(0)$	$f''(0)$	$\varphi'(0)$	$f''(0)$	$\varphi'(0)$
1.0	1.0	1.0	0	−0.5	−1.27088654	−1.423024	−1.197986	−1.439168	−0.63374633	−1.492982
				0	−1.03002477	−1.4448913	−1.00006318	−1.459439	−1.157468	−1.450724
				1	−0.60791487	−1.4801828	−0.63374637	−1.492982	−0.987383	−1.469818
			1.0	−0.5	−1.7755839	−1.372818	−1.59455919	−1.395419	−1.4802514	−1.415179
				0	−1.544125	−1.393875	−1.41421366	−1.414214	−1.333014	−1.429549
				1	−1.1198733	−1.4297158	−1.07219779	−1.446799	−1.0144068	−1.459888
Nsc	Gc_x	β	Mn	r	$f''(0)$	$\varphi'(0)$	$f''(0)$	$\varphi'(0)$	$f''(0)$	$\varphi'(0)$
1.0	−0.5	0.0	0.0	−1	−1.4744947	−0.0820259	−1.34098339	−0.154732	−1.26106811	−0.219564
				0	−1.42712963	−0.5024353	−1.29997051	−0.579856	−1.23105419	−0.625866
				1	−1.36961126	−0.9050402	−1.26890254	−0.941886	−1.20380557	−0.988173
			1.0	−1	−1.88961136	−0.1622099	−1.67625248	−0.226013	−1.53962576	−0.297629
				0	−1.86004245	−0.5275533	−1.65359342	−0.589658	−1.52245402	−0.651764
				1	−1.83595955	−0.8502349	−1.63945073	−0.891564	−1.50791633	−0.967822
		1.0	0.0	−1	−1.23887444	−0.8595579	−1.61953044	−0.874294	−1.50044334	−0.893634
				0	−1.21614492	−1.1653026	−1.6061051	−1.146077	−1.48954093	−1.165961
				1	−1.19842923	−1.4390568	−1.59442222	−1.395741	−1.48007047	−1.415839
			1.0	−1	−1.61958182	−0.8741826	−1.24077618	−0.860318	−1.19054615	−0.878865
				0	−1.60613751	−1.1459873	−1.21920943	−1.165234	−1.17238474	−1.180051
				1	−1.59444451	−1.395673	−1.2016108	−1.395741	−1.15745211	−1.450780

The effects of the modified Grashof number Gc_x and modified Schmidt number NSc on the concentration ϕ for shear-thinning ($n = 0.8$), Newtonian ($n = 1$), and shear-thickening ($n = 1.8$) fluids are shown respectively in Figs. 4a–4c. Increasing the value of Gc_x results in a decrease in the concentration boundary layer thickness, associated with an increase in the wall mass transfer gradient, and hence produces an increase in the surface mass transfer rate. Also the effects of species diffusion are found to be more pronounced for a fluid with smaller NSc. This is because the concentration gradient accelerates the dispersion of the species. This observation is true even in the cases of Newtonian and shear-thinning fluids. The concentration profiles ϕ across the flow field are plotted in Figs. 5a–5c for different values of the reaction rate parameter β and the wall concentration parameter r. From these graphs we observe that the effect of increasing the value of β is to decrease the concentration in the flow files. However, the values for the mass concentration are higher for negative values

Table 3
Wall mass transfer gradient for several sets of values of the physical parameters when $Gc_x = 0.0$.

Mn	*Nsc*	β	$n = 0.8$			$n = 1.0$			$n = 1.2$		
			$r = -1.0$	$r = 0.0$	$r = 1.0$	$r = -1.0$	$r = 0.0$	$r = 1.0$	$r = -1.0$	$r = 0.0$	$r = 1.0$
		−0.2	0.90761256	−0.28942246	−0.83988213	0.58243429	−0.33078056	−0.85106456	0.36460393	−0.37621986	−0.86234188
		−0.1	0.34465769	−0.44188919	−0.91819787	0.20788549	−0.47637686	−0.93244678	0.10837546	−0.50472128	−0.94202382
		0	0.08920488	−0.55124092	−0.98470843	−0.00033915	−0.58207011	−1.00002313	−0.87134725	−0.60523045	−1.00976384
	1.0	1	−0.82349992	−1.15792513	−1.44514358	−0.84998554	−1.17650056	−1.45944881	−1.30559862	−1.19081783	−1.46980393
		2	−1.27241611	−1.53486156	−1.77189296	−1.2906257	−1.54965055	−1.7844218	−1.63629973	−1.56129682	−1.7938714
		3	−1.60949111	−1.83439314	−2.04233384	−1.62416482	−1.84712112	−2.05369973	−2.15611053	−1.85723698	−2.0623672
	0.1		−0.28194680	−0.34656223	−0.40780244	−0.28932973	−0.35016116	−0.40483326	−0.30634031	−0.36300695	−0.41716154
0.0	1		−0.82349991	−1.15792513	−1.44514358	−0.84998554	−1.17650056	−1.45944881	−0.87134725	−1.19081783	−1.46980393
	2	1.0	−1.14159536	−1.6598 1936	−2.09094334	−1.18342769	−1.69003761	−2.11523294	−1.21724474	−1.71388197	−2.13382316
	3		−1.3839103	−2.04665422	−2.58868814	−1.43830121	−2.08585525	−2.62032247	−1.48225331	−2.11702991	−2.6449368
	5		−1.76652586	−2.66165519	−3.37980652	−1.84169507	−2.71503019	−3.42267656	−1.90230536	−2.75772333	−3.45646095
	0.1		−0.04023509	−0.13340851	−0.21801733	−0.07526443	−0.15488517	−0.22935866	−0.13848877	−0.20587134	−0.27014578
	1	0.0	0.089204878	−0.55124092	−0.98470843	−0.00033915	−0.58207011	−1.00002313	−0.00602143	−0.60523045	−1.00976384
	2		0.147762969	−0.85624301	−1.4903152	−2.25E−07	−0.91134691	−1.5231775	−0.10063229	−0.95189691	−1.5469923
	3		0.194991142	−1.09278643	−1.87935746	−0.58207012	−1.1652422	−1.92368007	−0.13264428	−1.21967959	−1.95709813
		−0.2	0.62351489	−1.26226413	−20.4149151	1.36310685	0.05617746	−0.59023941	0.455747485	−0.22778498	−0.71026397
		−0.1	0.434942693	−0.28075812	−0.75379717	0.263581187	−0.34918943	−0.79252827	0.131374359	−0.41221699	−0.82890964
		0	0.06764324	−0.46169049	−0.86242455	−0.00202396	−0.50226873	−0.89270198	−0.06402525	−0.53797114	−0.91733235
	1.0	1	−0.84685492	−1.13548303	−1.39387774	−0.86594897	−1.15501654	−1.41421354	−0.88223517	−1.17060935	−1.42952025
		2	−1.28818858	−1.5269105	−1.73629594	−1.30185902	−1.53627753	−1.75314164	−1.3137846	−1.54867315	−1.7660352
		3	−1.62154162	−1.82405996	−2.01458168	−1.63290274	−1.83723533	−2.02932715	−1.64279926	−1.84790754	−2.04070473
	0.1		−0.28998926	−0.33928378	−0.38713452	−0.29493758	−0.34358990	−0.390919	−0.31029075	−0.35746819	−0.40034775
1.0	1		−0.84685492	−1.13548303	−1.39387774	−0.86579489	−1.15501654	−1.41421354	−0.88223517	−1.17060947	−1.42952025
	2	1.0	−1.17017651	−1.63221478	−2.0322275	−1.20206463	−1.66383207	−2.06398249	−1.22955775	−1.68932939	−2.08846736
	3		−1.41534066	−2.01628423	−2.52648044	−1.45828748	−2.0572629	−2.56647944	−1.49509704	−2.09039617	−2.5975709
	5		−1.80120265	−2.62819552	−3.31407571	−1.86304319	−2.68390965	−3.36638784	−1.9155519	−2.72899437	−3.40733409
	0.1		−0.05371000	−0.11845974	−0.18028628	−0.08343126	−0.14339821	−0.20171341	−0.14362118	−0.19821523	−0.25114978
	1	0.0	0.06764324	−0.46169049	−0.86242455	−0.00020239	−0.50226873	−0.89270192	−0.06025290	−0.53798032	−0.91733235
	2		0.119924612	−0.75667787	−1.36416447	−1.46E−05	−0.82304465	−1.4142509	−0.08862627	−0.87315649	−1.45121884
	3		0.163366422	−0.98982388	−1.75277352	−1.01E−07	−1.0752157	−1.81591523	−0.11901872	−1.1400881	−1.86334813

of β as compared to positive values of β. Physically, $\beta < 0$ represents a generative chemical reaction, i.e., the species which diffuses from the stretching sheet is produced by a chemical reaction in the free stream, and $\beta > 0$ a destructive chemical reaction i.e., one that reduces the thickness of the concentration layer and increases the wall transfer, as shown in these figures. This behavior occurs for both zero and non-zero values of r. From the graphical representation we also observe that an increase in r leads a decrease in the concentration profile ϕ, and that the magnitude of the wall concentration gradient increases with the wall concentration. This is due to the fact that when $r > 0$ the species diffuses from the stretching sheet into the ambient medium and when $r < 0$ the species diffuses into the stretching sheet from the ambient medium.

The values of $-f''(0)$ and $-\phi'(0)$, respectively, which signify the local skin friction coefficient, C_f, and the mass transfer gradient, are recorded in Tables 2 and 3 for different values of the governing parameters. From Table 2, we observe that $-f''(0)$ increases with an increase in the magnetic field parameter Mn for various values of n. It is interesting to note that the magnitude of the wall surface gradient decreases gradually with increasing n and Gc_x. The effect of the power-law index on $-f''(0)$ is more significant in a shear-thinning fluid ($n < 1$) than in a shear-thickening fluid ($n > 1$). It is further noticed that the effect of n is to increase the magnitude of the wall mass transfer gradient whereas the reverse trend is seen with Mn. This result has a significant role in industrial applications to reduce the power supply expenditure by stretching the sheet just by increasing the magnetic parameter Mn. Further, it can be seen from Table 3 that the effects of increasing values of the reaction rate parameter β, wall concentration parameter r and the modified Schmidt number NSc are to decrease the mass transfer gradient at the wall.

5. Conclusion

In this work, we have explored the influence of the reaction rate parameter on the MHD flow and mass transfer of a power-law fluid over a stretching sheet. Similarity transformations are used to reduce the partial differential equations into ordinary differential equations. Numerical solutions for the velocity and species distribution are obtained for different values of the pertinent parameters using the Keller–Box method. Based on the computational results the new findings are as follows.

- The effect of increasing the values of the power-law index and the magnetic parameter is to reduce the fluid velocity profile and hence reduce the boundary layer thickness.
- The effect of the magnetic field is to enhance the wall mass transfer gradient and hence enhance the species distribution.
- An increase of the reaction rate parameter and wall concentration parameter reduces the thickness of the species distribution. This holds good for all values of the power-law index.
- An increase in the modified Grashof number enhances the velocity boundary layer thickness; whereas quite the opposite is true for the mass concentration.

Acknowledgments

The authors appreciate the comments of the reviewers, which have led to definite improvement in the paper. One of the authors, K.V. Prasad, expresses his grateful thanks to the DST authorities for providing financial support through a BOYSCAST fellowship.

References

[1] D.T. Chin, Mass transfer to a continuous moving sheet electrode, J. Electroanal. Chem. 122 (1975) 643–646.
[2] R.M. Griffith, Velocity, temperature and concentration distributions during fiber spinning, Ind. Eng. Chem. Fundam. 3 (1964) 245–250.
[3] B.C. Sakiadis, Boundary layer behavior on continuous solid surfaces: I. Boundary layer equations for two-dimensional and axisymmetric flow, AIChE J. 7 (1961) 26–28.
[4] F. Tsou, E. Sparrow, R.J. Goldstein, Flow and heat transfer in the boundary layer on a continuous moving surface, Int. J. Heat Mass Transfer 10 (1967) 219–235.
[5] L.J. Crane, Flow past a stretching plate, Z. Angew. Math. Phys. 21 (1970) 645–647.
[6] P.S. Gupta, A.S. Gupta, Heat and mass transfer on a stretching sheet with suction or blowing, Can. J. Chem. Eng. 55 (1977) 744–746.
[7] L.J. Grubka, K.M. Bobba, Heat transfer characteristics of a continuous stretching surface with variable temperature, Trans. ASME, J. Heat Transfer 107 (1985) 248–250.
[8] R. Cortell, Flow and heat transfer of a fluid through a porous medium over a stretching surface with internal heat generation/absorption and suction/blowing, Fluid Dynam. Res. 37 (2005) 231–245.
[9] R. Cortell, Internal heat generation and radiation effects on a certain free convection flow, Int. J. Nonlinear Sci. 9 (2010) 468–479.
[10] B. Vujannovic, A.M. Status, D.J. Djukiv, A variational solution of the Rayleigh problem for power law non-Newtonian conducting fluid, Ing. Arch. 41 (1972) 381–386.
[11] W.R. Schowalter, The application of boundary layer theory to power law pseudo plastic fluids: similar solutions, AIChE J. 6 (1960) 24–28.
[12] A. Acrivos, A theoretical analysis of laminar natural convection heat transfer to non-Newtonian fluids, AIChE J. 6 (1960) 584–590.
[13] S.Y. Lee, W.F. Ames, Similar solutions for non-Newtonian fluids, AIChE J. 12 (1966) 700–708.
[14] H.I. Andersson, B.S. Dandapat, Flow of a power law fluid over a stretching sheet, Stab. Appl. Anal. Contin. Media 1 (1991) 339–347.
[15] A.K. Sahu, M.N. Mathur, P. Chaturani, S.S. Bharatiya, Momentum and heat transfer from a continuous moving surface to a power law fluid, Acta Mech. 142 (2000) 119–131.
[16] K.B. Pavlov, Magnetohydrodynamic flow of an incompressible viscous fluid caused by deformation of a plane surface, Magnin. Gidrodinam. USSR 4 (1974) 146–147.
[17] A. Chakrabarti, A.S. Gupta, Hydromagnetic flow and heat transfer over a stretching sheet, Quart. Appl. Math. 37 (1979) 73–78.
[18] R. Cortell, A note on magneto hydrodynamic flow of power law fluid over a stretching sheet, Appl. Math. Comput. 168 (2005) 557–566.

[19] R. Cortell, MHD flow and mass transfer of an electrically conducting fluid of second grade in a porous medium over a stretching sheet with chemically reactive species, Chem. Eng. Process. 46 (2007) 721–728.
[20] K.V. Prasad, K. Vajravelu, Heat transfer in the MHD flow of a power law fluid over a non-isothermal stretching sheet, Int. J. Heat Mass Transfer 52 (2009) 4956–4965.
[21] M. Subhas Abel, P.S. Datti, N. Mahesha, Flow and heat transfer in a power law fluid over a stretching sheet with variable thermal conductivity and non-uniform heat source, Int. J. Heat Mass Transfer 52 (2009) 2902–2913.
[22] J.R. Fan, J.M. Shi, X.Z. Xu, Similarity solution of mixed convection with diffusion and chemical reaction over a horizontal moving plate, Acta Mech. 126 (1988) 59–69.
[23] D.F. Fairbanks, C.R. Wike, Diffusion and chemical reaction in an isothermal laminar flow along a soluble flat plate, Ind. Eng. Chem. Res. 42 (1950) 471–475.
[24] P.L. Chambre, J.D. Young, On the diffusion of a chemically reactive species in a laminar boundary layer flow, Phys. Fluids 1 (1958) 48–54.
[25] N. Dural, A.L. Hines, A comparison of approximate and exact solutions for homogeneous irreversible chemical reaction in the laminar boundary layer, Chem. Eng. Commun. 96 (1990) 1–14.
[26] H.I. Andersson, O.R. Hansen, B. Holmedal, Diffusion of chemically reactive species from a stretching sheet, Int. J. Heat Mass Transfer 37 (1994) 659–664.
[27] S.P.A. Devi, R. Kandaswamy, Effects of chemical reaction heat and mass transfer on MHD flow past a semi infinite plate, Z. Angew. Math. Phys. 80 (2000) 697–701.
[28] K.V. Prasad, M. Subhas Abel, P.S. Datti, Diffusion of chemically reactive species of a non-Newtonian fluid immersed in a porous medium over a stretching sheet, Internat. J. Non-Linear Mech. 38 (2003) 651–657.
[29] R. Cortell, Toward an understanding of the motion and mass transfer with chemically reactive species for two classes of viscoelastic fluid over a porous stretching sheet, Chem. Eng. Process. 46 (2007) 982–989.
[30] J.P. Denier, P.P. Dabrowski, On the boundary layer equations for power law fluids, Proc. R. Soc. Lond. Ser. A 460 (2004) 3143–3158.
[31] H.I. Andersson, K.H. Bech, B.S. Dandapat, Magnetohydrodynamic flow of a power law fluid over a stretching sheet, Internat. J. Non-Linear Mech. 27 (1992) 929–936.
[32] T. Cebeci, P. Bradshaw, Physical and Computational Aspects of Convective Heat Transfer, Springer-Verlag, New York, 1984.
[33] H.B. Keller, Numerical Methods for Two-point Boundary Value Problems, Dover Publ., New York, 1992.